JOURNAL OF SOLID STATE CHEMISTRY 44, 257–267 (1982)

The System $NiAl_2O_4$–Ni_2SiO_4 at High Pressures and Temperatures: Spinelloids with Spinel-Related Structures

MASAKI AKAOGI,*,† SYUN-ITI AKIMOTO,* KEIJI HORIOKA,‡
KEN-ICHI TAKAHASHI,‡,§ AND HIROYUKI HORIUCHI‡,||

*Institute for Solid State Physics, University of Tokyo, Roppongi,
Minato-ku, Tokyo 106, and ‡Institute of Scientific and Industrial Research,
Osaka University, Suita, Osaka 565, Japan

Received March 19, 1982

Phase relations in the system $NiAl_2O_4$–Ni_2SiO_4 were studied in the pressure range 1.5 ~ 13.0 GPa and in the temperature range 800 ~ 1450°C. Two new phases, IV and V, were found in regions of pressure higher than 4 GPa. Phase V disproportionates into a mixture of Ni_2SiO_4-spinel, NiO, and Al_2O_3 at approximately 9.5 GPa and 1100°C. Phases III, IV, and V form a solid solution in some compositional range: phases IV and V have a composition around $NiAl_2O_4 \cdot Ni_2SiO_4$, whereas phase III spreads from $NiAl_2O_4 \cdot Ni_2SiO_4$ to the $NiAl_2O_4$-rich side. All the phases I ~ V are structurally considered to be spinel derivatives, "spinelloids," with three kinds of tetrahedral groups; isolated tetrahedra TO_4, linked ones T_2O_7, and triply linked ones T_3O_{10}. The ratios of isolated tetrahedra to linked ones are large in the higher-pressure phases and small in the lower-pressure phases. The difference of compositional range of phase III from that of phases IV and V is possibly explained by the avoidance of linked tetrahedra such as O_3–Al–O–Al–O_3.

Introduction

The olivine(α)–spinel(γ) phase transformation of M_2TO_4 compounds at high pressures and high temperatures has been extensively investigated not only for interest in their crystal–chemical properties but also for application to solid-state behavior of the Earth's interior. During the course of studies on phase transformations of nearly iron-free $(Mg,Fe)_2SiO_4$, Ringwood and Major (*1*) observed the presence of an intermediate phase between the α and γ phases. This intermediate phase was confirmed as a stable phase in the studies of phase transformations of Co_2SiO_4 (*2*) and Mn_2GeO_4 (*3*).

Crystal structure studies of the intermediate phases of Mn_2GeO_4 (*4*) and $(Mg_{0.9}Ni_{0.1})_2SiO_4$ (*5*) revealed that the structures were closely related to the spinel structure, therefore these intermediate phases were designated as "modified spinel" or "β-phase." Recently, the structure of pure β-Mg_2SiO_4 has also been precisely studied (*6*).

It is of interest to search for other possible intermediate phases between α and γ phases under high-pressure and high-temperature conditions. Ma (*7*) investigated the

---

|| To whom correspondence should be addressed.

† Present address: Department of Chemistry, Arizona State University, Tempe, Arizona 85237.

§ Present address: Research and Development Department, Daini Seikosha Co., Ltd., Kameido 6-31-1 Koto-ku, Tokyo 136, Japan.

0022-4596/82/110257-11$02.00/0

phase equilibria of the pseudobinary system $NiAl_2O_4$–Ni_2SiO_4 at pressures up to 4 GPa in the temperature range 1000 ~ 1700°C. In the system $NiAl_2O_4$–Ni_2SiO_4, one end member $NiAl_2O_4$ crystallizes in the spinel structure at atmospheric pressure, whereas the other, Ni_2SiO_4, directly transforms from the olivine to the spinel structure at approximately 3 GPa at 1000°C. He found three new phases in the system $NiAl_2O_4$–Ni_2SiO_4 besides α and γ phases which were denoted as phases I, II, and III. The compositions of these three phases are represented by $3NiAl_2O_4 \cdot Ni_2SiO_4$ (phase I), $3NiAl_2O_4 \cdot 2Ni_2SiO_4$ (phase II), and $NiAl_2O_4 \cdot Ni_2SiO_4$ (phase III). The structure studies indicated that phases II (*8*) and III (*9*) are isostructural with *manganostibite*, Mn_7SbAsO_{12} (*10*), and with the β phase, respectively, and phase I (*11*) is a new spinel-related structure which has isolated tetrahedra TO_4 and triply linked tetrahedra T_3O_{10} in it.

Two new phases, IV and V, with approximate composition $NiAl_2O_4 \cdot Ni_2SiO_4$ were found in the recent investigation on the phase relations of the system $NiAl_2O_4$–Ni_2SiO_4 at higher pressure than that used by Ma (*7*). Structure analyses on these new phases indicated that they are interpreted as a hybrid structure of spinel and β-phase structures (*12, 13*), both of which have isolated tetrahedra TO_4 and linked tetrahedra T_2O_7 in the structures. In a previous paper (*14*), the aforementioned phases I ~ V were structurally summarized as "*spinelloids*" and the relationship between structure and stability pressure was discussed.

In this study, the phase relations in the system $NiAl_2O_4$–Ni_2SiO_4 were examined in the pressure range 1.5 ~ 13.0 GPa and in the temperature range 800 ~ 1450°C. A pressure–temperature stability diagram is determined for the bulk composition of $NiAl_2O_4 \cdot Ni_2SiO_4$. Furthermore, an isothermal section of the synthesis diagram of the high-pressure phases in the $NiAl_2O_4$–Ni_2SiO_4 system is presented at 1100°C, and the interrelationship among pressure, structure, and composition is also discussed.

Experimental

1. High-pressure and high-temperature apparatus. High-pressure and high-temperature experiments were carried out by means of two types of high-pressure apparatus: a tetrahedral–anvil type and a double-staged cubic–octahedral–anvil type in the Institute for Solid State Physics, University of Tokyo. The former type of apparatus was used for the experiments in the pressure range 1.5 ~ 9.5 GPa; the latter for the experiments at 8.2 ~ 13.0 GPa. In the runs with the tetrahedral–anvil type, four different sizes of anvils with triangle faces 9, 15, 20, and 25 mm in edge were used together with pressure medium pyrophyllite tetrahedra 14, 20, 25, and 30 mm in edge, respectively. In the experiments with the cubic–octahedral apparatus, a 2.5-mm-edge octahedral anvil was used in combination with a 7-mm-edge octahedron made of semisintered polycrystalline MgO. A detailed description of this cubic–octahedral apparatus was given by Akaogi and Akimoto (*15*).

Pressure values in these multianvil apparatuses were estimated by a calibration curve which was obtained in advance from the relationship between the press load and the electric resistivity change at several pressure-fixed points such as Bi I–II(2.55 GPa), Ba I–II(5.5 GPa), Bi III–V(7.7 GPa), and Ba II–III(12.6 GPa) based on the NBS scale (*16*) and Akimoto *et al.* (*17*).

In most of the experimental runs, a platinum cylindrical foil was used as a furnace and the starting materials were placed directly in it. Graphite cylindrical heaters were also used for some of the runs at temperatures higher than 1100°C, because the platinum heaters were often burned off at high temperatures. In this case, samples were charged into a platinum capsule in order to avoid reduction of the sample due to the reducing atmosphere at the elevated temperatures. The capsule was covered with a pyrophyllite sleeve, and then placed into the graphite heater. Temperatures were measured by Pt/Pt–13% Rh thermocouples which were placed in contact with the outside of the platinum capsule or the platinum heater. No corrections were made for the effects of pressure on the electromotive force of the thermocouple.

2. *Starting materials.* In this study, three kinds of starting materials were used: (1) mixtures of synthetic Ni_2SiO_4(olivine) and $NiAl_2O_4$(spinel), (2) mixtures of NiO, $Al(OH)_3$, and silicic acid, and (3) mixtures of each component of (2) preheated at 700°C for about 30 min. The starting materials (1) were used in most runs for the equimolar composition of $NiAl_2O_4$ and Ni_2SiO_4. Ni_2SiO_4(olivine) was prepared by heating a mixture of NiO and silicic acid in appropriate composition at 1300°C for 202 hr. $NiAl_2O_4$(spinel) was synthesized from the equimolar mixture of NiO and Al_2O_3 at 1420°C for 48 hr. In some runs, a small amount of water was added to (1) to increase the reaction rate. In the runs for growing single crystals large enough for the structure analyses of the phases in the system $NiAl_2O_4$–Ni_2SiO_4, the starting materials (2) were adopted. The starting materials (3) were used in order to avoid the effects of water on the phase equilibrium studies, and they were also used in the runs of compositions with $m\mathrm{NiAl_2O_4} \cdot n\mathrm{Ni_2SiO_4}$ ($m:n$ = 3:1, 3:2, 2:3, and 1:3).

3. *Identification of phases and chemical compositions.* Normal quenching technique was applied to obtain desired specimens in this experiment. The sample was held at an appropriate pressure–temperature condition for enough time to be in equilibrium, the temperature was rapidly decreased to room temperature by turning off the heating power, and finally the applied pressure was released. All the quenched products were examined by X-ray powder diffraction with Cu$K\alpha$ radiation. Single crystals of products were examined by conventional X-ray camera methods in order to obtain crystallographic data.

An analytical electron microscope (AEM) in the Institute of Scientific and Industrial Research, Osaka University, was also used to identify the phases of the products. We can get information on the chemical compositions and the diffraction patterns simultaneously for an area smaller than 1 μm by AEM. We used specimens which were prepared as thin as possible in order to avoid the systematic errors due to the thickness of the specimen. Standard materials, such as Ni_2SiO_4(olivine), $NiAl_2O_4$(spinel), Al_2SiO_5(kyanite), and anorthite with a composition Ab_5An_{95}, were used to calibrate the cation ratios and the ratios of integrated characteristic X-ray intensities from cations. Energy analyses of Al and Si of specimens 1 (phase IV) and 2 (phase V) and their electron diffraction patterns are shown with the X-ray spectrum of Al_2SiO_5 in Fig. 1. Characteristic X-ray spectra in Fig. 1 indicate the same Si/Al ratios for all materials, and the electron diffraction patterns show that the periodicities along b^* are different between specimens 1 and 2.

Results and Discussion

1. *Results*

Experimental results are summarized into two groups as follows: (1) determination of the phase relations of the composition fixed to $NiAl_2O_4 \cdot Ni_2SiO_4$ in the pressure and temperature ranges 1.5 ~ 13.0 GPa and 800 ~ 1450°C, respectively, and (2) determination of the phase relations of various compositions with $m\mathrm{NiAl_2O_4} \cdot n\mathrm{Ni_2SiO_4}$ ($m:n$ = 3:1, 3:2, 2:3, and 1:3) at

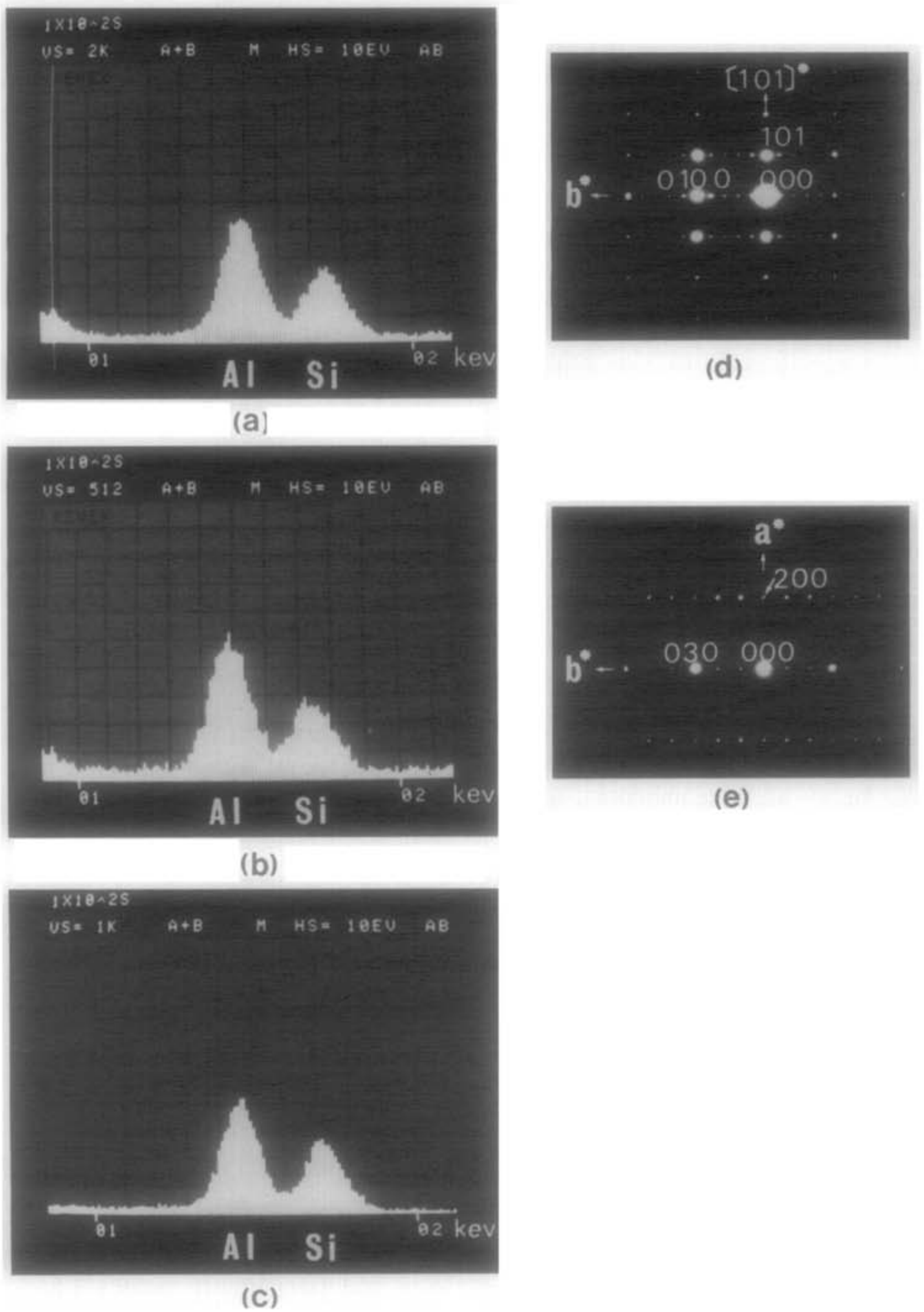

FIG. 1. Comparison of characteristic X-ray spectra from phases IV (a) and V (b) of nickel aluminosilicates and kyanite (Al_2SiO_5) (c). Kyanite was used as a standard specimen. Electron diffraction patterns of phases IV (d) and V (e) are also shown.

temperatures of 1100 ~ 1330°C and in the pressure range 3.8 ~ 7.2 GPa.

The results of each run in the cases of (1) and (2) are listed in Tables I and II, respectively. In this work, two new phases, designated as phases IV and V, were found. In addition to these phases, phases II and III, olivine, silicate spinel, aluminate spinel, NiO, and Al_2O_3 were also observed. Phases II and III observed in this study were confirmed to be identical to phases II and III, respectively, reported by Ma (*7*) by means of the X-ray diffraction method.

2. *Crystal–Chemical Properties of Phases IV and V*

Crystals of phases IV and V are transparent and green, and show low birefringence under the petrographic microscope. The optical properties are quite similar to those of phase III. X-ray powder diffraction patterns of phases IV and V give strong subcell reflections which are related to the spinel structure, and these characteristics are also seen in the diffraction patterns of phases I, II, and III. However, the features of extra reflections are quite different among these five phases as shown in Fig. 2, so that each phase is easily distinguished. Crystal data of phases I ~ V are summarized in Table III. The result of structure analysis of each phase was reported as shown in the references of Table III.

3. *Pressure–Temperature Diagram of* $NiAl_2O_4 \cdot Ni_2SiO_4$

A synthesis diagram of high-pressure polymorphs for the composition $NiAl_2O_4 \cdot Ni_2SiO_4$ is illustrated in Fig. 3. In the present experimental condition, phases II, III, IV, and V were observed, in addition to olivine and spinel phases, NiO, and Al_2O_3. In the pressure range 1.5 ~ 3.0 GPa at temperatures 1080 ~ 1440°C, the two-phase assemblage of phase II plus olivine-type phase was observed. At higher pressures, this assemblage transforms to a

TABLE I

RESULTS OF RUNS FOR THE BULK COMPOSITION OF $NiAl_2O_4 \cdot Ni_2SiO_4$

Run No.	Pressure (GPa)	Temperature (°C)	Time (min)	Phases
92	1.5	1190	60	Ol + II
90	1.7	1320	20	II + Ol
64	1.9	1220	20	II + Ol
55[b]	2.1	1080	90	II + Ol
70	2.2	1300	15	II + Ol
84[a]	2.3	1260	20	II + Ol
31[b]	2.5	1130	50	III + Ol + II
54[b]	2.6	1060	60	III
29	2.6	1190	40	III + Ol + II
28	2.7	1290	30	III + II + Ol
83[a]	2.8	1230	30	II + III + Ol
58	3.0	1440	15	II + III + Ol
53[a]	3.1	1060	30	III
63	3.2	1200	25	III
57	3.4	1440	15	III
21	3.5	1300	20	III
27[b]	3.7	850	120	III
34	3.8	1150	60	III
50[b]	3.8	1270	15	III
61	3.9	1400	10	III
8	4.0	930	90	III
16	4.4	1070	45	III
41[a]	4.6	1220	25	III
48[a]	4.6	1450	10	III
17	4.7	1060	80	III
703	5.0	900	240	III
619	5.5	1180	60	III
20	5.6	1070	90	III + IV
35	5.8	1270	20	III + IV
107[b]	6.1	900	90	IV
611[a]	6.5	1280	20	IV
106[a]	6.6	900	120	IV
42	7.0	1420	10	IV
99	7.1	1100	45	IV
39	7.2	940	80	IV
38	7.3	1080	30	IV + V (tr)
36	7.4	1270	20	V + IV
704	8.2	1000	55	V
95	8.6	1260	10	V
97	9.3	1100	20	V
96	9.5	1260	15	V
705	9.7	1050	20	S.Sp + Cor + NiO
428	10.0	900	60	S.Sp + Cor + NiO
424	13.0	800	70	S.Sp + Cor + NiO
427	13.0	850	50	S.Sp + Cor + NiO

Note. Starting materials: [a] NiO + $Al(OH)_3$ + silicic acid; [b] Ni_2SiO_4 (olivine) + $NiAl_2O_4$ (spinel) + H_2O; others, Ni_2SiO_4 (olivine) + $NiAl_2O_4$ (spinel). Phases: II, III, IV, and V, phases II ~ V of nickel–aluminosilicates; Ol, Ni_2SiO_4 (olivine); S.Sp, Ni_2SiO_4 (spinel); Cor, Al_2O_3.

TABLE II

RESULTS OF RUNS FOR THE BULK COMPOSITIONS OF $m\mathrm{NiAl_2O_4} \cdot n\mathrm{Ni_2SiO_4}$ WITH $m:n$ = 3:1, 3:2, 2:3, AND 1:3

Run No.	Bulk composition (m/n)	P (GPa)	T (°C)	Time (min)	Phases
37	3	4.0	1100	60	Sp + III (tr)
39	3	5.0	1100	60	IV + Sp
41	3	6.1	1100	60	IV + Sp
53	3	6.5	1100	60	IV + Sp (tr)
44	3 .	6.9	1100	60	IV + Sp
9[a]	3	6.3	1250	10	Sp + IV (tr)
12[a]	3	5.2	1260	35	Sp + IV
5[a]	3	6.0	1300	10	IV + Sp
47	$\frac{3}{2}$	3.8	1100	60	III + Sp
49	$\frac{3}{2}$	5.0	1100	60	IV + III
15[a]	$\frac{3}{2}$	5.5	1100	25	IV
51	$\frac{3}{2}$	6.0	1100	60	IV
45	$\frac{3}{2}$	7.2	1100	60	IV
16[a]	$\frac{3}{2}$	5.0	1200	15	IV + III (tr)
48	$\frac{2}{3}$	3.8	1100	60	III + X_p + X
50	$\frac{2}{3}$	5.0	1100	60	IV + X (tr)
52	$\frac{2}{3}$	6.0	1100	60	III + IV + S.Sp + X (tr)
46	$\frac{2}{3}$	7.2	1100	60	V + S.Sp + X
25[a]	$\frac{2}{3}$	4.0	1250	30	III + IV
24[a]	$\frac{2}{3}$	5.0	1300	30	IV + III
22[a]	$\frac{2}{3}$	6.1	1300	30	IV + III + X_p
23[a]	$\frac{2}{3}$	7.0	1300	30	IV + Gl
38	$\frac{1}{3}$	4.0	1100	60	III + X_p
40	$\frac{1}{3}$	5.0	1100	60	III + S.Sp
42	$\frac{1}{3}$	6.1	1100	60	III + S.Sp (tr) + X_p (tr)
54	$\frac{1}{3}$	6.5	1100	60	S.Sp + X
43	$\frac{1}{3}$	6.9	1100	60	S.Sp + X
42	$\frac{1}{3}$	6.1	1250	60	III + S.Sp (tr) + X_p (tr)
29[a]	$\frac{1}{3}$	6.0	1320	30	III + X_p
20[a]	$\frac{1}{3}$	7.0	1320	30	V + III (tr) + Gl (tr)
26[a]	$\frac{1}{3}$	4.0	1330	30	III + X_p

Note. Starting materials: [a] marked runs, mixtures of NiO, $\mathrm{Al(OH)_3}$, and silicic acid; others, mixtures of above heated at 700°C for 30 min. Phases: III, IV and V, phases III ~ V of nickel–aluminosilicates: Sp, $\mathrm{NiAl_2O_4}$ (spinel): S.Sp, $\mathrm{Ni_2SiO_4}$ (spinel); Gl, glass; X and X_p, unknown phases (see text).

single phase III. These results are consistent with the study by Ma (*7*), except that the transformation pressure of this work is a little higher than that reported by Ma. This discrepancy may be attributed to the decrease of pressure in the pyrophyllite cell at high temperature above 1000°C in the case of using a multianvil apparatus, as suggested by Akimoto *et al.* (*18*). Phase III transforms to phase IV at the approximate pressure 5.5 GPa, and phase IV further transforms to phase V at 7.0 GPa. At the pressure 9.5 GPa, phase V decomposes into a mixture of $\mathrm{Ni_2SiO_4}$ (spinel type), NiO (rock salt type), and $\mathrm{Al_2O_3}$ (corundum). A spinel solid solution with the composition

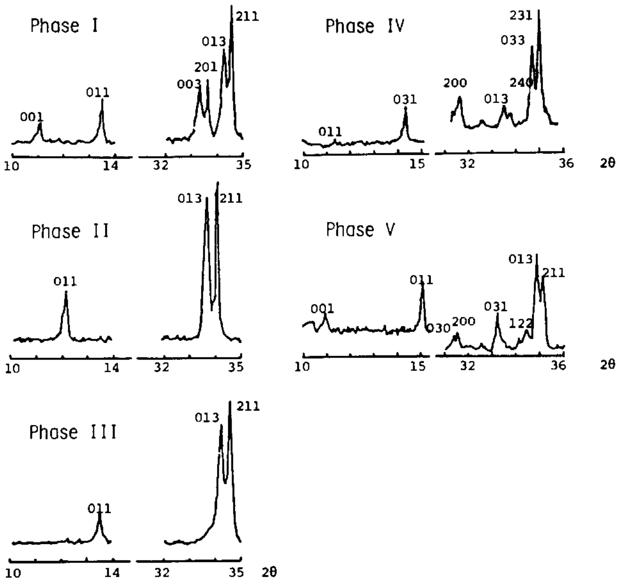

FIG. 2. Comparison of X-ray powder diffraction patterns among phases I ~ V of nickel aluminosilicates. Patterns of phases I and II were quoted from the experimental results of Ma (*7*). β-filtered CuKα radiation was used.

$NiAl_2O_4 \cdot Ni_2SiO_4$ was not observed in this experiment. This disproportionation might be closely related to the decomposition of $NiAl_2O_4$ (spinel) into NiO and Al_2O_3, which was reported by Ringwood and Reid (*19*).

Each phase of I ~ V has a narrow compositional range as discussed in the following section in detail. Therefore, two-phase fields of $III_{s.s} + IV_{s.s}$ and $IV_{s.s} + V_{s.s}$ should exist in the phase diagram of Fig. 3 for the composition $NiAl_2O_4 \cdot Ni_2SiO_4$. The two-phase fields are tentatively added in Fig. 3.

Using the cell constants, density increases accompanying the following phase transformations or reactions:

$$\underset{\text{phase II}}{3NiAl_2O_4 \cdot 2Ni_2SiO_4} + \underset{\text{olivine}}{Ni_2SiO_4} \rightarrow \underset{\text{phase III}}{3[NiAl_2O_4 \cdot Ni_2SiO_4]},$$

$$\underset{\text{phase III}}{NiAl_2O_4 \cdot Ni_2SiO_4} \rightarrow \underset{\text{phase IV}}{NiAl_2O_4 \cdot Ni_2SiO_4},$$

$$\underset{\text{phase IV}}{NiAl_2O_4 \cdot Ni_2SiO_4} \rightarrow \underset{\text{phase V}}{NiAl_2O_4 \cdot Ni_2SiO_4},$$

TABLE III

CRYSTAL DATA FOR PHASES I ~ V

Phase	Compositions ($NiAl_2O_4$/Ni_2SiO_4)	*a* (Å)	*b* (Å)	*c* (Å)	Space group	Density	Ref.
I	3	5.6664(5)	11.496(2)	8.0983(7)	*Pmma*	4.69	(*11*)
II	$\frac{3}{2}$	5.6603(7)	17.298(2)	8.110(1)	*Imma*	4.78	(*8*)
III	1	5.665(2)	11.483(2)	8.100(2)	*Imma*	4.87	Present work
IV	1	5.665(2)	28.646(9)	8.091(9)	*Imma*	4.900	(*12*)
V	1	5.665(1)	8.590(1)	8.097(2)	*Pmma*	4.907	(*13*)

Note. Values in parentheses of lattice constants are standard deviations.

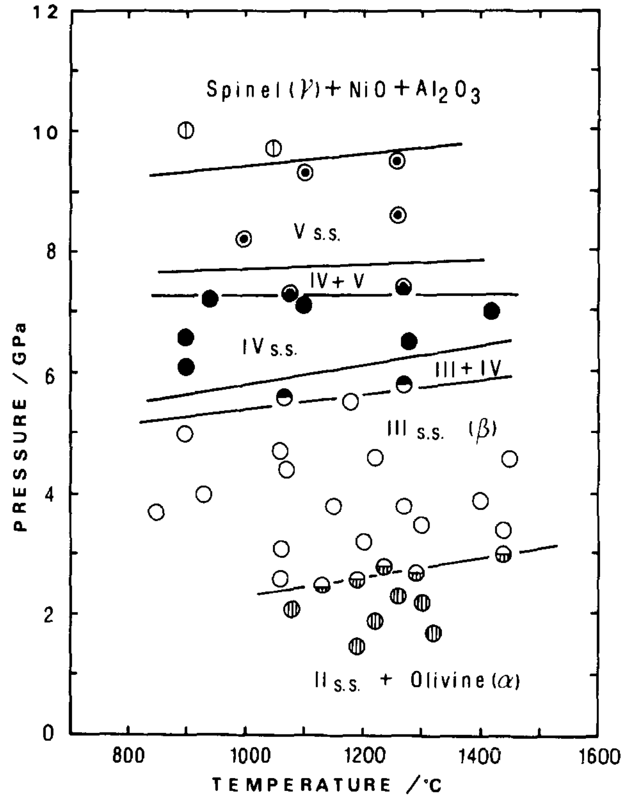

FIG. 3. A pressure–temperature diagram for the synthesis of the high-pressure phases of the bulk composition of $NiAl_2O_4 \cdot Ni_2SiO_4$. Notations are shown in Table I.

$$\underset{\text{phase V}}{NiAl_2O_4 \cdot Ni_2SiO_4} \rightarrow \underset{\text{spinel}}{Ni_2SiO_4} + \underset{\text{rock salt}}{NiO} + \underset{\text{corundum}}{Al_2O_3},$$

are calcuated to be 1.7, 0.6, 0.2, and 3.9%, respectively, where the lattice constants for phases I ~ V are from Table III and those for Ni_2SiO_4 olivine and spinel are from the data reported by Akimoto *et al.* (*20*).

4. *Pressure–Composition Diagram of the System $NiAl_2O_4$–Ni_2SiO_4*

A pressure–composition diagram for the synthesis of the high-pressure phases in the system $NiAl_2O_4$–Ni_2SiO_4 at 1100°C is shown in Fig. 4. The data points in Fig. 4 were partially collected from Tables I and II. The phases which were observed in the runs with various bulk compositions are the same as those found in the experiments with the composition $NiAl_2O_4 \cdot Ni_2SiO_4$ in the previous section, except for unknown phases assigned as X and X_p in Table II.

Chemical compositions of phases III, IV, and V, silicate spinel, and aluminate spinel in six typical run products, which were evaluated by means of AEM, are listed in Table IV. The results indicate that phases III, IV, V, silicate spinel, and aluminate spinel have a compositional range as a solid solution in the pseudobinary system $NiAl_2O_4$–Ni_2SiO_4. Phase boundaries in Fig. 4 were schematically represented on the basis of phase assemblages and the chemical composition of each phase in the run products. In this diagram, phase relations at pressures lower than 3 GPa and

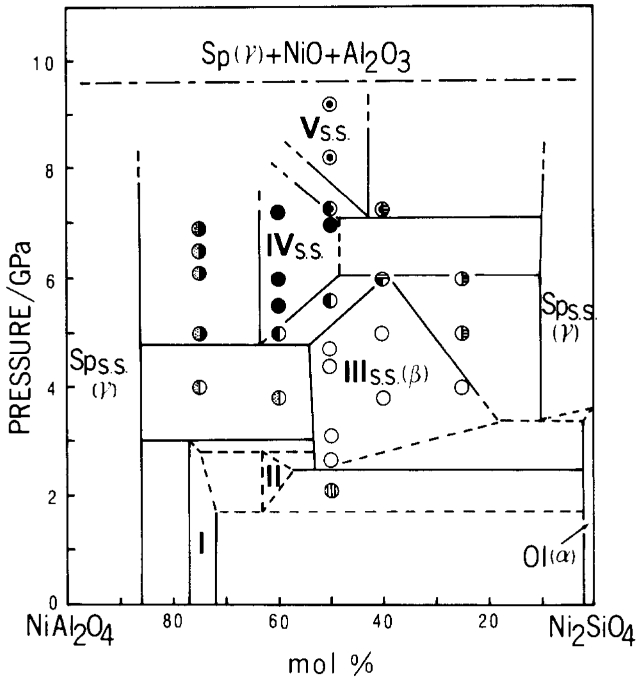

FIG. 4. A schematic pressure–composition diagram for the synthesis of the high-pressure phases in the system $NiAl_2O_4$–Ni_2SiO_4 at approximately 1100°C. Notations are shown in Table II.

higher than 8 GPa are based on the results by Ma (7) and those described in the previous section, respectively. Phases III, IV, and V have a fairly wide compositional range, and a region of each phase is separated by a two-phase field. Therefore, it will

TABLE IV

CHEMICAL COMPOSITIONS OF COEXISTING PHASES OF SEVERAL TYPICAL RUN PRODUCTS

Run No.	Bulk composition $NiAl_2O_4 \cdot Ni_2SiO_4$	P (GPa)	T (°C)	Phase	Composition of each phase
40	1:3	5.0	1100	III	$0.28NiAl_2O_4 \cdot 0.72Ni_2SiO_4$
				S.Sp.	$0.10NiAl_2O_4 \cdot 0.90Ni_2SiO_4$
42	1:3	6.1	1100	III	$0.39NiAl_2O_4 \cdot 0.61Ni_2SiO_4$
				S.Sp.	$0.10NiAl_2O_4 \cdot 0.90Ni_2SiO_4$
52	2:3	6.0	1100	IV	$0.50NiAl_2O_4 \cdot 0.50Ni_2SiO_4$
				III	$0.39NiAl_2O_4 \cdot 0.61Ni_2SiO_4$
				S.Sp.	$0.10NiAl_2O_4 \cdot 0.90Ni_2SiO_4$
46	2:3	7.0	1100	V	$0.40NiAl_2O_4 \cdot 0.60Ni_2SiO_4$
				S.Sp.	$0.08NiAl_2O_4 \cdot 0.92Ni_2SiO_4$
37	3:1	4.0	1100	Sp.	$0.86NiAl_2O_4 \cdot 0.14Ni_2SiO_4$
				III	$0.46NiAl_2O_4 \cdot 0.54Ni_2SiO_4$
44	3:1	6.9	1100	Sp.	$0.88NiAl_2O_4 \cdot 0.12Ni_2SiO_4$
				IV	$0.56NiAl_2O_4 \cdot 0.44Ni_2SiO_4$

Note. Phase: III, IV and V, phases III ~ V of nickel aluminosilicates; S.Sp., silicate spinel; Sp., aluminate spinel. Standard deviations for compositions are approximately 0.05.

be reasonable to consider that the crystallographic relationship among phases III, IV, and V is not polymorphism.

Small amounts of phases assigned as X and X_p were often observed only in the run products obtained under hydrous conditions with SiO_2-rich compositions. X-Ray microanalysis spectra from the phases X and X_p by means of AEM indicated that the phases contained trace or no Ni and were rich in Si and/or Al. The X-ray powder diffraction patterns and the chemical compositions of the phases X and X_p suggested that these phases were related to layered aluminosilicate, but the details are still unknown.

5. Crystal Structure and Its Relation to Phase Diagram

Crystal structures of phases IV and V were reported by Horioka *et al.* (*12, 13*) and that of phase III by Ma and Sahl (*9*). These studies indicate that phase III is isostructural to the modified spinel, and phases IV and V crystallize into hybrid structures of modified spinel and spinel. Both structures of phases IV and V are constructed from an isolated tetrahedron TO_4 and a linked group T_2O_7, being accompanied by a single column and a double column of MO_6 octahedra. The ratios of TO_4 to T_2O_7 in the structures of phases IV and V are 1:2 and 1:1, respectively. In phase III, only the T_2O_7 group is observed.

TABLE V

TETRAHEDRAL GROUPS IN THE STRUCTURES I ~ V AND THE APPROXIMATE PRESSURE AND COMPOSITION RANGES OF THEIR STABILITY FIELDS

Phase	TO_4	T_2O_7	T_3O_{10}	Composition $(x)^a$	Stability pressure (GPa)
I	1		1	~ 0.25	0.0 ~ 2.5
II			1	~ 0.60	2.0 ~ 2.5
III		1		0.25 ~ 0.50	2.5 ~ 6.0
IV	1	2		0.50 ~ 0.60	5.0 ~ 7.2
V	1	1		0.45 ~ 0.50	7.0 ~ 9.5

[a] Compositions are given by $x(NiAl_2O_4) \cdot (1 - x)Ni_2SiO_4$.

The structure of phase I (*11*) contains both TO_4 and T_3O_{10} and phase II contains only T_3O_{10}. The tetrahedral groups in phases I ~ V are summarized in Table V together with their pressure and composition ranges. If we assume a "*basic structural unit*" in the spinel structure, which is constructed from a TO_4 tetrahedron and an MO_6 octahedron, all the structures of phase I ~ V can be represented by one-dimensional arrangements of the *unit* along the *b* axes. The arrangements of the *unit* along the *a* and *c* axes are the same as that of spinel. Thus, these phases I ~ V can be considered to be spinel derivatives, and were systematized as "*spinelloids*" (*14*).

The ratios of isolated tetrahedra in the structures are systematically increased in the phases stable at high pressures. This tendency is especially clear in phases III, IV, and V. Phase V decomposes into a mixture of silicate spinel, NiO, and Al_2O_3, in which the T_2O_7 group is not found but only TO_4 is observed. The oxygen packings in the structures should become more ideal under higher-pressure conditions in order to increase their densities. Strong intercation repulsive forces between linked tetrahedra like T_2O_7 or T_3O_{10} cause the oxygen packing to distort and this distortion will be disadvantageous for the structure to be dense under high-pressure conditions. Therefore, the ratio of isolated tetrahedra in the structures will be increased in higher-pressure phases.

As shown in Fig. 4, the stability region of phase III deviates from the $NiAl_2O_4 \cdot Ni_2SiO_4$ composition to the Ni_2SiO_4-rich side. This can be explained by the avoidance of linked tetrahedra like $O_3-Al-O-Al-O_3$ in the structure, because phase III contains only linked tetrahedra T_2O_7 and both of the T's cannot be occupied by Al ions. On the other hand, compositional ranges of phases IV and V can spread to the $NiAl_2O_4$-rich side, because they contain both isolated TO_4 and linked T_2O_7, and both TO_4 and one of the T's of T_2O_7 can be occupied by Al ions. In fact, the results of the structural analyses of phases IV and V reveal that Al ions are relatively concentrated in isolated tetrahedra (*12*, *13*).

In contrast to the $NiAl_2O_4$–Ni_2SiO_4 system, "spinelloids" with spinel-related structures do not occur in the system $FeAl_2O_4$–Fe_2SiO_4 and $CoAl_2O_4$–Co_2SiO_4 (*21*). In these systems, $M_3Al_2Si_3O_{12}$ (M = Fe and Co) garnet phases appear in the phase assemblages. The occurrence of spinelloids in the system $NiAl_2O_4$–Ni_2SiO_4 might be related to the instability of $Ni_3Al_2Si_3O_{12}$ garnet.

Acknowledgments

We thank Professors N. Morimoto and M. Tokonami for their helpful discussions, and also Mr. T. Tanaka for his help with the electron microscopic work. The experiments of high-pressure and high-temperature syntheses were supported by a Research Board Grant of the Institute for Solid State Physics, University of Tokyo.

References

1. A. E. Ringwood and A. Major, *Earth Planet. Sci. Lett.* **1,** 241 (1966).
2. S. Akimoto and Y. Sato, *Phys. Earth Planet. Inter.* **1,** 498 (1968).
3. S. Akimoto, *Phys. Earth Planet. Inter.* **3,** 189 (1970).
4. N. Morimoto, S. Akimoto, K. Koto, and M. Tokonami, *Phys. Earth Planet. Inter.* **3,** 161 (1970).
5. P. B. Moore and J. V. Smith, *Phys. Earth Planet. Inter.* **3,** 166 (1970).
6. H. Horiuchi and H. Sawamoto, *Amer. Mineral.* **66,** 568 (1981).
7. Che-Bao Ma, *Contrib. Mineral. Petrol.* **45,** 257 (1974).
8. Che-Bao Ma and E. Tillmanns, *Acta Crystallogr. Sect. B* **31,** 2139 (1975).
9. Che-Bao Ma and K. Sahl, *Acta Crystallogr. Sect. B* **31,** 2142 (1975).
10. P. B. Moore, *Amer. Mineral.* **55,** 1489 (1970).
11. Che-Bao Ma, K. Sahl, and E. Tillmanns, *Acta Crystallogr. Sect. B* **31,** 2137 (1975).
12. K. Horioka, K. Takahashi, N. Morimoto, H. Horiuchi, M. Akaogi, and S. Akimoto, *Acta Crystallogr. Sect. B* **37,** 635 (1981).
13. K. Horioka, M. Nishiguchi, N. Morimoto, H. Horiuchi, M. Akaogi, and S. Akimoto, *Acta Crystallogr. Sect. B* **37,** 638 (1981).
14. H. Horiuchi, M. Akaogi, and H. Sawamoto, *in* "High-Pressure Research in Geophysics" (S. Akimoto and M. H. Manghnani, Eds.), Center for Academic Publ. Japan, Tokyo (1982).
15. M. Akaogi and A. Akimoto, *Phys. Earth Planet. Inter.* **15,** 90 (1977).
16. E. C. Lloyd, "Accurate Characterization of the High-Pressure Environment," *Nat. Bur. Stand. Spec. Publ.* **326,** 313 (1971).
17. S. Akimoto, T. Yagi, Y. Ida, K. Inoue, and Y. Sato, *High Temp. High Pressures* **7,** 287 (1975).
18. S. Akimoto, T. Yagi, and K. Inoue, *in* "High-Pressure Research: Applications in Geophysics" (M. H. Manghnani and S. Akimoto, Eds.), Academic Press, New York (1977).
19. A. E. Ringwood and A. F. Reid, *Earth Planet. Sci. Lett.* **5,** 245 (1968).
20. S. Akimoto, Y. Matsui, and Y. Syono, *in* "The Physics and Chemistry of Minerals and Rocks" (P. G. J. Strens, Ed.), Wiley, New York/London (1976).
21. E. Ohtani and H. Sawamoto, *Mineral J.* **8,** 226 (1976).